Redox Biology 16 (2018) 322–331

Contents lists available at ScienceDirect

Redox Biology

journal homepage: www.elsevier.com/locate/redox

Research Paper

Copper accumulation in senescent cells: Interplay between copper transporters and impaired autophagy

Shashank Masaldan[a,b,*], Sharnel A.S. Clatworthy[a], Cristina Gamell[c], Zoe M. Smith[d], Paul S. Francis[d], Delphine Denoyer[a], Peter M. Meggyesy[a], Sharon La Fontaine[a,b,1], Michael A. Cater[a,e,**,1]

[a] Centre for Cellular and Molecular Biology, School of Life and Environmental Sciences, Deakin University, Burwood, Victoria 3125, Australia
[b] The Florey Institute of Neuroscience and Mental Health, Parkville, Victoria 3052, Australia
[c] Peter MacCallum Cancer Centre, Melbourne, Victoria 3000, Australia
[d] School of Life and Environmental Sciences, Deakin University, Geelong, Victoria 3220, Australia
[e] Department of Pathology, The University of Melbourne, Parkville, Victoria 3010, Australia

ARTICLE INFO

Keywords:
Senescence
Copper
Ageing
Homeostasis
Autophagy

ABSTRACT

Cellular senescence is characterized by irreversible growth arrest incurred through either replicative exhaustion or by pro-oncogenic cellular stressors (radioactivity, oxidative stress, oncogenic activation). The enrichment of senescent cells in tissues with age has been associated with tissue dyshomeostasis and age-related pathologies including cancers, neurodegenerative disorders (e.g. Alzheimer's, Parkinson's, etc.) and metabolic disorders (e.g. diabetes). We identified copper accumulation as being a universal feature of senescent cells [mouse embryonic fibroblasts (MEF), human prostate epithelial cells and human diploid fibroblasts] *in vitro*. Elevated copper in senescent MEFs was accompanied by elevated levels of high-affinity copper uptake protein 1 (Ctr1), diminished levels of copper-transporting ATPase 1 (Atp7a) (copper export) and enhanced antioxidant defence reflected by elevated levels of glutathione (GSH), superoxide dismutase 1 (SOD1) and glutaredoxin 1 (Grx1). The levels of intracellular copper were further increased in senescent MEFs cultured in copper supplemented medium and in senescent Mottled Brindled (Mo^{br}) MEFs lacking functional Atp7a. Finally, we demonstrated that the restoration/preservation of autophagic-lysosomal degradation in senescent MEFs following rapamycin treatment correlated with attenuation of copper accumulation in these cells despite a further decrease in Atp7a levels. This study for the first time establishes a link between Atp7a and the autophagic-lysosomal pathway, and a requirement for both to effect efficient copper export. Such a connection between cellular autophagy and copper homeostasis is significant, as both have emerged as important facets of age-associated degenerative disease.

1. Introduction

Cellular senescence represents a critical barrier against cellular transformation and prevents the uncontrolled proliferation of cells that are irrevocably damaged [13,63]. Senescent cells actively secrete a variety of proteins, including pro-inflammatory mediators (cytokines and chemokines) to elicit immunological self-clearance [13,73]. Other secreted factors facilitate communication with the local microenvironment and can establish senescence in neighbouring cells in a paracrine manner [50,53]. The beneficial roles of senescent cells, for instance in wound healing, tissue remodelling and against cancer development, are considered conditional on their efficient and timely tissue clearance [13,73]. However, senescent cells accumulate in tissues and organs with age and contribute to age-related pathologies and dysfunction, in part, through promoting chronic inflammation [13,73]. Why senescent cells accumulate with age is unclear, but it is likely to be associated with age-associated immunodeficiency and therefore reduced clearance [17,54,67,74]. Recently developed strategies to clear senescent cells *in vivo* have provided remarkable improvement to the healthspan of mice by attenuating age-related pathologies and tissue dysfunctions [2–4,16,77].

We previously provided an aetiological link between senescent cell

* Correspondence to: Melbourne Dementia Research Centre, The Florey Institute of Neuroscience and Mental Health, The University of Melbourne, 30 Royal Parade, Parkville, VIC 3052, Australia.
** Correspondence to: Centre for Cellular and Molecular Biology, School of Life and Environmental Sciences, Deakin University, 221 Burwood Highway, Burwood, VIC 3125, Australia.
E-mail addresses: shashank.masaldan@florey.edu.au, shashank.masaldan@deakin.edu.au (S. Masaldan), mcater@deakin.edu.au, mcater@unimelb.edu.au (M.A. Cater).
[1] Co-senior authors.

https://doi.org/10.1016/j.redox.2018.03.007
Received 28 January 2018; Received in revised form 9 March 2018; Accepted 13 March 2018
Available online 17 March 2018

enrichment and iron dyshomeostasis, both of which occur in tissues with ageing and at sites of age-related pathologies [44]. We demonstrated that senescent cells accumulate substantial amounts of intracellular iron (up to 30-fold) as a consequence of impaired ferritinophagy (ferritin degradation) [44]. Elevated ferritin proved to be a robust biomarker for cellular senescence, for associated iron accumulation and for resistance to iron-induced toxicity, including ferroptosis. [44]. In this study, we further investigated whether other biologically relevant metals are altered in cellular senescence and identified a consistent increase in intracellular copper. Several groups have previously reported that elevated copper (250–500 μM) induces premature senescence in certain cell types [e.g. human diploid fibroblasts and fetal lung fibroblasts] [8,41,47,48,60], which can be attenuated by the copper chelator resveratrol [6,48,69]. Furthermore, replicative senescent human diploid fibroblasts (HDFs) have been shown to accumulate copper (2-fold) [8] and harbour increased mRNA transcript levels for copper-regulated genes, *heat shock protein 70*, *metallothionein 2A* and *prion protein* [60]. We hypothesized that copper accumulation is a feature of cellular senescence and investigated the cellular modifications that potentially contributed to elevated copper levels, such as enhanced antioxidant mechanisms and alterations to key copper homeostasis proteins. Further, we describe the key role of lysosomal dysfunction in senescence-associated copper accumulation.

2. Experimental

2.1. Chemicals and reagents

Rapamycin was purchased from Thermo Fischer Scientific (Cat#FSBBP2963-1). Bafilomycin A1 (Baf A1) (Cat# B1793) was purchased from Sigma Aldrich. All other reagents were purchased from Sigma Aldrich unless otherwise stated.

2.2. Isolation and culturing of primary mouse and human cells

Primary mouse embryonic fibroblasts (MEFs) were collected from sacrificed pregnant mice [C57BL/6 wild-type, Li-Fraumeni syndrome C57BL/6, agouti, mottled brindle (Mo^{br}) mice] at 13 day post-*coitum* and cultured as described previously [44]. Li-Fraumeni syndrome leads to a predisposition to tumor development in individuals that carry inherited mutations in tumor suppressor gene *TP53* [39]. The Li-Fraumeni syndrome C57BL/6 mice, that harbour a *TP53* germline mutation (G515A nucleotide mutation), were a kind gift from Prof. Guillermina Lozano (University of Texas) [39]. This study was approved by the Deakin University Animal Ethics Committee (AEC) (Id#G01–2014). Primary human diploid fibroblasts (HDFs) (S103) obtained from the Murdoch Children's Research Institute, Melbourne, and human primary prostate epithelial cells (PrECs), purchased from Lonza (Cat#CC-2555) were cultured as described previously [44].

2.3. Screening of MEFs carrying copper-transporting ATPase 1 (Atp7a)-Mo^{br} mutation

MEFs were screened for presence of *Atp7a-*Mo^{br} mutation by polymerase chain reaction (PCR) as described previously [42]. Briefly, sense oligonucleotides MMNK22 (5'-GGCAAAACCTCCGAGGCAAAG) specific for *Atp7a-*Mo^{br} mutation or MMNK23 (5'- CAAAACCTCCGAGGCTCT TGC) specific for wild-type *Atp7a* and antisense oligonucleotide MMNK24L (5'-AGGAGGAGATTTTCAGAGTTCAG-3') were used to amplify products of 83 bp and 87 bp, respectively, in separate reaction tubes. PCR conditions were as follows: 96 °C for 4 min, 63 °C for 1 min, 72 °C for 1 min for two cycles followed by 96 °C for 1 min, 63 °C for 1 min, 72 °C for 30 s for 35 cycles. The PCR products were resolved on a 4% agarose (agarose 3:1 High Resolution Blend, AMRESCO) gel and detected by staining with ethidium bromide.

2.4. Senescence induction by ionizing radiation

Senescence was induced in primary mouse and human cell lines (MEFs, HDFs and PRECs) as previously described [44]. Briefly, cells were cultured to ~ 90% confluence in 25 or 75 cm^2 flasks (Cellstar®, Cat#690175 or 658175, respectively) and subjected to 10 Gray (Gy) gamma irradiation using a calibrated Cesium-137 source (Gamma Cell 40, Atomic energy of Canada Limited). Cellular senescence was assessed at appropriate time points (in days) post-irradiation by senescence-associated β-galactosidase (SA-βgal) activity staining, as detailed in the Results.

2.5. Retrovirus production and transduction of primary MEFs

HEK293T cells were cultured in DMEM medium supplemented with 10% FBS, penicillin (20 U/mL) and streptomycin (20 μg/mL), and were used as a packaging cell line for retrovirus production used for transduction of MEFs as described previously [44]. To produce retrovirus containing the SV40 Large T antigen (SV40 LgT), equimolar amounts of pBabe-neo large TcDNA plasmid (Addgene, Cat#1780) along with the packaging plasmid pCl-Eco (Addgene, Cat#12371) were used. Retrovirus containing the oncogene *H-Ras*^{V12} was produced with pWZL-Hygro H-*Ras* V12 plasmid (Addgene, Cat#18749), while control retrovirus was produced with empty pWZL-Hygro plasmid (Addgene, Cat#18750).

2.6. Senescence-associated β-galactosidase assay in cells

SA-βgal staining of cultured cells was performed as previously described [44]. The percentage of cells stained for SA-βgal activity was determined using an inverted microscope (Olympus IX51), by counting cells in four random fields of view at a magnification of 200/400X. Images were taken with Canon 1100D digital camera.

2.7. Western blotting analyses

Cell lysates were prepared and fractionated as described previously [44]. Gel fractionated protein samples were transferred to nitrocellulose membrane using Bolt® transfer system and buffer containing Tris-HCl (25 mM), glycine (192 mM) and 15% methanol (5% for Atp7a). Membranes were blocked for 1 h at room temperature using 5% (w/v) skimmed milk in wash (TBS-T) buffer containing Tris-HCl [10 mM (pH 8.0), NaCl (150 mM) and 0.1% Tween-20]. The following antibody dilutions were used: anti-CCS (Cat#FL274, 1:1000) was purchased from Santa Cruz Biotechnology, USA. Anti-β-actin (Cat#A5441, 1:10000), anti-LC3B (Cat#L7543, 1:1000) and HRP conjugated anti-goat IgG (Cat#A5420, 1:5000) were purchased from Sigma Aldrich. Anti-high-affinity copper uptake protein 1 (Ctr1) (Cat#EPR7936, 1:1000) and anti-Grx1 (Cat#AB16877, 1:1000) were purchased from Abcam. Anti-SOD1 (ADI-SOD-100, 1:2000) was purchased from Enzo Lifesciences, USA. Anti-Atp7a (R17, 1:500), goat polyclonal, was raised in-house and affinity purified. HRP conjugated goat-anti-mouse (Cat#P0447) and goat-anti-rabbit (Cat#P0448) antibodies were purchased from Dako. The membranes were subsequently developed using ECL reagent (Millipore, Cat#WBKLS0500) and bands visualized on Gel Dock™ XR + system (Bio-Rad). At least three independent experiments were used for all comparisons.

2.8. Determination of total intracellular copper

Total copper concentration was measured by inductively coupled plasma mass spectrometry (ICP-MS, Agilent 7700, Varian). Tissue culture cells were prepared for ICP-MS analyses as previously described [44]. Unit conversions from raw ppb values were performed as follows: (ng/million cells) = (raw ppb values × dilution factor/cell number).

2.9. Total glutathione determination

Reduced (GSH) and oxidized (GSSG) glutathione were measured by HPLC with permanganate chemiluminescence detection using a GloCel detector with serpentine flow-cell [49,66,71]. Cell pellets were homogenized (vortexed) in 300 μL of 0.1% formic acid and then centrifuged at 5000 × *g* at 4 °C for 15 min. For GSH determination, the supernatant was diluted 10-fold in aqueous formic acid (5%) immediately prior to analysis. For GSSG determination a second aliquot of the supernatant (100 μL) was combined with 20 μL of 675 mM Tris-HCl buffer (pH 8.0) and 20 μL of 6.3 mM *N*-ethylmaleimide (NEM) to block endogenous GSH, and mixed for 30 s. Then 20 μL of 8 mM 2-mercaptoethanol was added and mixed for a further 30 s. Subsequent to adding 20 μL of 780 nM TCEP, the solution was gently heated at 50 °C for 60 min to allow complete disulfide bond reduction. Finally, 20 μL of aqueous formic acid (5%) was introduced to re-acidify the sample prior to analysis.

2.10. Cell size determination

The diameter of suspended cells was determined by using a Coulter Z2 Cell Count and Size Analyser, as described previously [44].

2.11. Statistical and image analyses

Statistical analyses were performed using student-*t*-tests, using GraphPad PRISM (version 6.0b) software. All data are represented as mean ± SD; probabilities of $p < 0.05$ were considered significant.

3. Results and discussion

3.1. Senescent cells accumulate intracellular copper

We initially investigated whether cellular senescence is associated with altered copper homeostasis using primary mouse embryonic fibroblasts (MEFs) [23,44]. Senescence was induced by either sub-lethal gamma irradiation (10 Gy) or replicative exhaustion as described previously [44] and was confirmed through staining for senescence-associated beta-galactosidase (SA-βgal) activity (Fig. 1**A**). Note that primary MEFs underwent replicative exhaustion at passage 7 under our culturing conditions. More than 80% of MEFs stained positive for SA-βgal activity when cultured for a minimum of 10 days following either mode of senescence induction (Fig. 1**A**). Senescent cells remain metabolically active in culture for many months [44,73] and we therefore maintained senescent MEFs for 21 days to allow for a net change in intracellular copper to occur (Fig. 1**B**). Both irradiated (MEF IR) and replicative senescent (MEF REP) MEFs accumulated a significant amount of copper (~ 3–4-fold, respectively) when compared to primary proliferative MEFs (MEF PRI) (Fig. 1**B**). Variation in cell diameter (suspended), or total cellular protein content, between senescent (irradiated and replicative) and primary MEFs could not account for the degree of increased intracellular copper (Fig. 1**C**). Senescence induction and maintenance in murine cells is reliant on wild-type p53 function, the loss of which can result in senescence bypass/immortalization [24,31,73]. Both irradiation and replicative exhaustion lead to senescence induction through p53-mediated DNA damage response (DDR) pathways [73]. Accordingly, primary MEFs isolated from mice harbouring mutant p53 (G515A nucleotide mutation), which impairs senescence induction by irradiation [39,44], accumulated negligible amounts of intracellular copper post-irradiation (10 Gy) (Fig. 1**D**). Therefore, copper accumulation concomitant with senescence required wild-type p53 function and was not indirectly caused by irradiation. Likewise, wild-type MEFs that we aided to spontaneously bypass senescence using the 3T3 culturing method [ISO(3T3)] [72], had intracellular copper levels (Fig. 1**E**) comparable to primary MEFs (isogenic) (P4) (Fig. 1**F**). Note that senescence-bypass in MEFs commonly occurs through mutation of p53, leading to immortalization [30,59]. Therefore, copper accumulation in MEFs was not sustained following senescence bypass. Furthermore, MEFs immortalized with SV40 large T (LT) antigen (MEF LT) (Fig. 1**G**) and cultured also had intracellular copper levels comparable to primary MEFs (MEF PRI) (Fig. 1**F**). Thus, accumulation of copper was a feature of senescent MEFs (IR or REP) and was absent in primary and senescence bypassed/immortalized MEFs.

Oncogenes such as $HRas^{V12}$ can transform immortalized cells making them tumourigenic, but can also induce senescence in primary (non-immortalized) cells [63]. Oncogene-induced senescence (OIS) is distinct from irradiation and replicative-induced senescence and shares similar features with programmed developmental senescence [18,33,67]. We therefore transduced primary MEFs with $HRas^{V12}$ and verified senescence induction through SA-βgal activity staining at 8 days post-transduction (MEF OIS) (Fig. 1**H(i)**). Oncogene-induced ($HRas^{V12}$) senescent MEFs (MEF OIS) accumulated intracellular copper when compared to MEFs transduced with control retrovirus (MEF VC) (Fig. 1**H(ii)**), despite the limited percentage of senescent cells (> 50%). In contrast, immortalized MEFs transduced with retrovirus containing $HRas^{V12}$ (MEF LT Ras) had slightly reduced intracellular copper levels (Fig. 1**H(ii)**), demonstrating that $HRas^{V12}$ expression alone does not cause copper accumulation. Taken together, these results demonstrate that copper accumulated specifically in MEFs following senescence induction through irradiation (10 Gy), replicative exhaustion, or the $HRas^{V12}$ oncogene.

We further demonstrated that human primary diploid fibroblast (HDFs) and human prostate epithelial cells (PrECs), analogous to MEFs, also accumulated intracellular copper following senescence induction through irradiation (IR) (Fig. 1**I**). Therefore, our results demonstrate that intracellular copper accumulates in senescent cells irrespective of stimuli or cell origin and is therefore likely to represent a universal feature.

3.2. Copper accumulation in senescent cells is associated with altered copper homeostatic mechanisms

We investigated the levels of key cellular copper homeostasis proteins in senescent MEFs (21 days post-irradiation) (Fig. 2**A**). Western blot analyses revealed that senescent MEFs (MEFs IR) had significantly elevated levels of the high-affinity copper-uptake protein 1 (Ctr1), the principle protein responsible for the cellular uptake of copper (Fig. 2**A**). Ctr1 is the major copper import protein and resides as a trimeric complex that creates a pore through the plasma membrane (Fig. S1**A**) [40]. The transmembrane P_{1B}-type ATPase Atp7a in most cells (e.g. fibroblasts and epithelial cells) facilitates removal of excess copper across the plasma membrane [52,55]. The expression of Atp7a was significantly reduced in senescent MEFs (21 days post-irradiation) (Fig. 2**A**), which, in combination with elevated Ctr1, potentially contributed to their net increase in intracellular copper. Analogous changes to Ctr1 and Atp7a were also observed in replicative senescent MEFs (Fig. S1**B**). There was no change in *Atp7a* transcript levels post senescence induction (not shown), making it likely that the reduced Atp7a protein levels were a consequence of post-translational mechanisms, such as selective degradation via the ubiquitin-proteasome pathway [21,22,46]. Conceivably, the increase in intracellular copper in senescent cells would necessitate numerous adaptive changes by the cell to prevent toxicity from the production of reactive oxygen species (ROS). Therefore, we next investigated the levels of known antioxidants that afford cellular protection against copper-induced oxidative stress. Superoxide dismutase 1 (SOD1) scavenges superoxide anions, utilizes copper as a cofactor [76] and is a reliable marker of cellular stress [1]. SOD1 was markedly elevated in senescent MEFs (21 days post-irradiation) (Fig. 2**B**). The level of the copper chaperone for SOD1 (CCS) [62,76] remained unchanged suggesting that accumulated copper may be present in a bound state possibly sequestered by proteins (e.g.

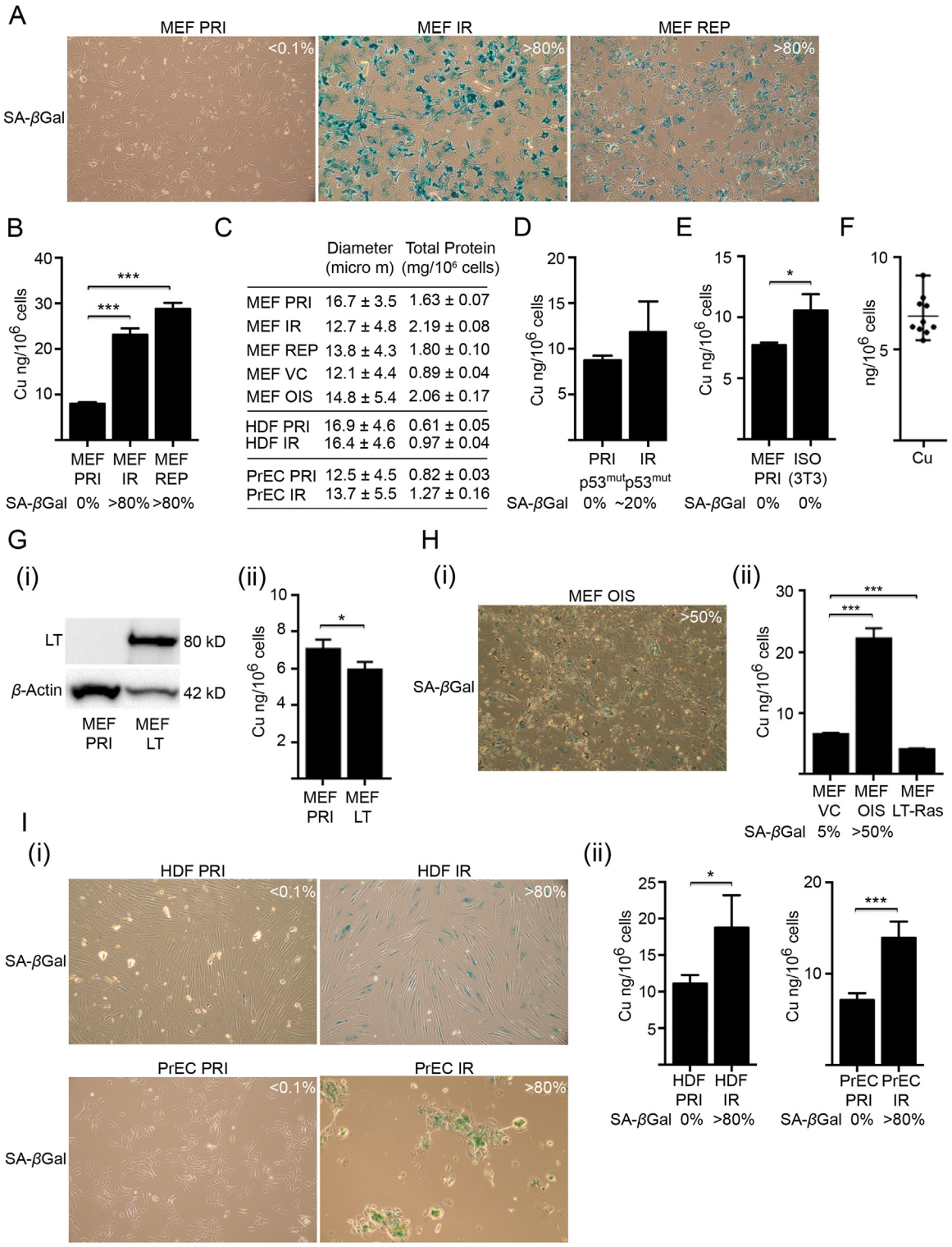

(caption on next page)

glutaredoxins, metallothioneins) or cytosolic antioxidants [e.g. glutathione (GSH)] (Fig. 2**B**) [5]. Glutaredoxin 1 (Grx1) is a GSH-dependent thiol-oxidoreductase that protects cellular proteins from oxidative damage by catalysing the reversible oxidation of protein thiols by GSSG to form mixed disulfides (P-SSG) (glutathionylation) or intramolecular disulfides (P-SS) [9,11,32]. Grx1 was previously shown to protect cells from copper-induced toxicity [15,65]. When the oxidative challenge is removed Grx1 may then catalyse the reverse reactions (deglutathionylation, reduction of intramolecular disulfide bonds) [11]. Analogous to SOD1, Grx1 expression is markedly elevated in senescent MEFs (21 days post-irradiation) (Fig. 2**B**). Grx1 also was demonstrated to bind copper with high affinity [11] and potentially could bind the accumulated copper. GSH as the major cellular antioxidant, is rich in the cytosol (1–10 mM) [25] and may be reversibly oxidized to its disulfide form GSSG. The GSSG/GSH couple constitutes a redox buffer that controls the redox status of cellular protein thiols among other

Fig. 1. Senescent cells accumulate copper. **(A)** Primary (non-immortalized) mouse embryonic fibroblasts (MEFs) were induced to senescence by either sub-lethal gamma irradiation (10 Gy) or replicative exhaustion. Senescent cell population in culture was determined through staining for senescence-associated beta-galactosidase (SA-βgal) activity (blue staining). Note that primary MEFs underwent replicative exhaustion at passage 7 under our culturing conditions. More than 80% of MEFs stained positive for SA-βgal activity when cultured for a minimum of 10 days following either mode of senescence induction. Images were taken at 100X magnification. **(B)** Induction of senescence in MEFs caused intracellular copper accumulation. ICP-MS analyses demonstrated that senescent MEFs (MEF IR) accumulated intracellular copper (~ 3-fold) at 21 days post-irradiation. Similarly, replicative senescent MEFs (MEF REP) when cultured for 21 days at passage 7 also accumulated intracellular copper (~ 4-fold). **(C)** Changes in cell mass and volume of senescent cells did not account for copper accumulation. Diameters of senescent cells in suspension (post-trypsinization) were found to be comparable to that of their primary precursor cells in suspension. Suspended cell diameter was determined by Beckman Coulter Z Series Cell Count and Size Analyser ($n = 3$) for all cell types being studied. Cellular protein content as a marker for overall cell mass and volume was determined for all cell types under study. Senescent irradiated (MEF IR) and senescent replicative MEFs (MEF REP) contained ~ 1.3-fold and ~ 1.1-fold more protein when compared to primary MEFs (MEF PRI), respectively. Oncogene induced senescent MEFs (MEF OIS) contained ~ 2.3-fold more protein than primary MEFs treated with control viral particles (MEF VC). Senescent human prostate epithelial cells (PrEC IR) and senescent human diploid fibroblasts (HDF IR) contained ~ 1.5-fold more protein than primary PrECs (PrEC PRI) and HDFs (HDF PRI), respectively. Note that in each case the senescence associated fold change in copper content was higher than the fold change in total cellular protein content. Cellular protein concentrations were determined using the BCA protein assay kit (Thermo Scientific) as per manufacturer's instructions. Total protein was determined as mg per 10^6 cells and represented as mean ± SD ($n = 3$). **(D)** Copper accumulation in irradiated MEFs was concomitant with senescence, was p53-driven and was not indirectly caused by irradiation. Primary MEFs isolated from mice harbouring mutant p53 (G515A nucleotide mutation), which impairs senescence induction by irradiation, displayed no significant increase in intracellular copper post-irradiation (10 Gy). Note that less than 20% of irradiated MEFs harbouring mutant p53 (IR $p53^{mut}$) stained positive for SA-βgal activity when cultured for a minimum of 10 days following irradiation. **(E)** Senescence bypass in MEFs by 3T3 subculture caused a limited increase in intracellular copper accumulation within the normal range of intracellular Cu in MEFs (see Fig. 1**F**). ICP-MS analyses demonstrated that isogenic MEFs, which spontaneously bypassed senescence [ISO (3T3)], had intracellular copper levels comparable to that of primary MEFs (MEF PRI). **(F)** Natural variance in intracellular copper in primary MEFs between different embryonic linages. ICP-MS analyses of isogeneic C57BL/6 MEF lines ($n = 10$) showed a range of intracellular Cu (5.9–9.0 ng/10^6 cells) concentrations. Data represented as mean ± range ($n = 10$). **(G)** Senescence bypass in MEFs by immortalization caused no increase in intracellular copper. **(i)** Primary MEFs were immortalized by transduction with retrovirus containing the SV40 large T antigen (LT) confirmed through western blot analyses. **(ii)** ICP-MS analyses demonstrated that immortalized MEFs (MEF LT) at passage 7 had intracellular copper levels comparable to that of primary MEFs (MEF PRI). **(H)** Induction of senescence in MEFs with virus containing the oncogene *H-Ras*^{V12} caused intracellular copper accumulation. **(i)** Primary MEFs transduced with virus containing *H-Ras*^{V12} (OIS) were enriched for SA-βgal positive cells (~ 50% at 8 days post-transduction) in comparison to primary MEFs transduced with control virus (VC) (~ 5%, not shown). **(ii)** ICP-MS analyses demonstrated that oncogene-induced senescent MEFs (OIS) accumulated intracellular Cu (~ 3.5-fold) at 8 days post-transduction with virus containing *H-Ras*^{V12}. Immortalized MEFs transduced with virus containing *H-Ras*^{V12} (MEF LT Ras) had intracellular copper levels comparable to that of primary MEFs (PRI) and significantly lower than MEF VC. **(I)** Induction of senescence by sub-lethal gamma irradiation (10 Gy) caused intracellular copper accumulation in human diploid fibroblast (HDFs) and human prostate epithelial cells (PrECs). **(i)** The majority (> 80%) of HDFs and PrECs displayed positive SA-βgal activity 10 days post-irradiation. **(ii)** ICP-MS analyses demonstrated that senescent HDFs (HDF IR) and senescent PrECs (PrEC IR) accumulated 1.7-fold and 2-fold more copper, respectively at 21 days post-irradiation compared to their respective non-irradiated primary cell. Statistical analysis was performed by student-*t*-test: significant ($*p < 0.05$, $**p < 0.01$, $***p < 0.001$). Data represented as mean ± SD ($n = 3$) unless stated otherwise.

antioxidative functions [61]. GSH has also been shown to play an important intermediary role in handling intracellular copper immediately following cellular uptake by Ctr1 [19,20,43] and may also mediate the loading of copper onto SOD1 through a CCS-independent mechanism [34,76]. GSH may bind the majority of cytosolic copper and can allow cells to accommodate elevated levels of copper while mitigating associated oxidative damage [27,5]. Furthermore, the level and ratio of GSH to GSSG can often serve as an indicator of the cellular redox status [61]. Since oxidative stress is a well-characterized feature of senescent cells [28,36], coupled with a marked increase in copper levels, we postulated that changes to the levels of GSH and the GSH/GSSG ratio would likely occur in senescent cells. In senescent MEFs (21 days post-irradiation) there was a substantial increase in both reduced GSH (~ 5-fold) and oxidized GSSG (~ 7-fold), combined with a lower ratio of GSH:GSSG (Fig. 2**C**). Replicative senescent MEFs showed similar changes in GSH and GSSG levels (Fig. S1**C**). Taken together, these results demonstrate that copper accumulation in senescent cells is associated with changes in the expression profile of relevant copper homeostatic proteins. Furthermore, a concomitant increase in major cellular antioxidants, SOD1, Grx1 and GSH, may protect senescent cells against the adverse effects of oxidative stress. In the case of GSH and Grx1, this protection may occur through mechanisms that include the binding or sequestering of accumulated copper.

3.3. Dose-dependent copper accumulation in senescent MEFs is exacerbated in the absence of Atp7a

Senescent cells remain metabolically active and undergo morphological and biochemical changes correlating with different phases in their progression [73]. We therefore determined whether the degree of copper accumulation in senescent MEFs reflected the duration of time in culture and/or the availability of copper in the extracellular milieu. Copper accumulation was monitored in irradiated MEFs following different time periods in culture (1, 7, 14 and 21 days) (Fig. 3**A**). Note that the medium was replenished weekly for each time point. Intracellular copper accumulated in irradiated cultures and correlated with the increasing percentage of senescent cells at each time point (Fig. 3**A**). However, the level of accumulated copper somewhat plateaued but was maintained after day 14, indicating that an upper threshold may have been reached (Fig. 3**A**). Similarly, MEFs undergoing replicative exhaustion progressively accumulated intracellular copper in accordance with the percentage of senescent cells at each passage, reaching an upper limit when cells at passage 7 were cultured for 10 days (Fig. 3**B**). Further culturing of replicative senescent MEFs (21 days) did not augment copper accumulation (Fig. 3**B**). To establish whether these apparent upper thresholds were dependent on milieu copper, we treated both irradiated (14 days post-irradiation) and replicative senescent MEFs (passage 7 cultured for 10 days) with either basal medium or media supplemented with 20 μM $CuCl_2$ for 24 h (Fig. 3**C**). Note that primary proliferative MEFs (passage 4) were treated equivalently as a control (Fig. 3**C**). In medium supplemented with 20 μM $CuCl_2$ there was an increase in the capacity of senescent MEFs (IR and REP) to accumulate intracellular copper (Fig. 3**C**). The reason for the higher copper accumulation in irradiated senescent MEFs compared to replicative senescent MEFs is currently unclear.

We next investigated the importance of Atp7a activity on the extent of copper accumulation in senescent cells. We utilized the brindled mouse mutant (*Mo*^{br}) that most closely models Menkes disease (MD), an X-linked recessive copper-deficiency disorder caused by mutation(s) in the *ATP7A* gene (human orthologue of mouse *Atp7a*) [29]. *Mo*^{br} mice harbour a 6 base-pair deletion (GCTCTT from nucleotides 2473–2478) in *Atp7a*, resulting in the in-frame deletion of two amino acids; an alanine residue (Ala799) and a highly conserved leucine residue (Leu800). While cells and tissue from *Mo*^{br} mice display normal levels of Atp7a transcript and protein, the protein fails to efficiently mediate copper efflux [29,37]. Analogous to human MD fibroblasts, several cell types isolated from *Mo*^{br} mice, such as lung fibroblasts, kidney epithelial cells and fetal cells were reported to harbour elevated copper (~ 4-fold, ~ 7-fold and ~ 21-fold, respectively) when compared to counterpart normal cells in culture [12]. We generated MEFs from *Mo*^{br} and agouti (same background as *Mo*^{br}: wt*Atp7a*) mouse embryos and subsequently irradiated them to induce cellular senescence. We established that 10 days following irradiation, more than 80% of MEFs from both *Mo*^{br} (MEF-Mo^{br}) and agouti [MEF (A)] mice stained positive for SA-βgal activity (Fig. 3**D(i)**), analogous to MEFs from the C57BL/6 background (Fig. 1**A**). Both irradiated *Mo*^{br} (MEF-Mo^{br}) and agouti [MEF

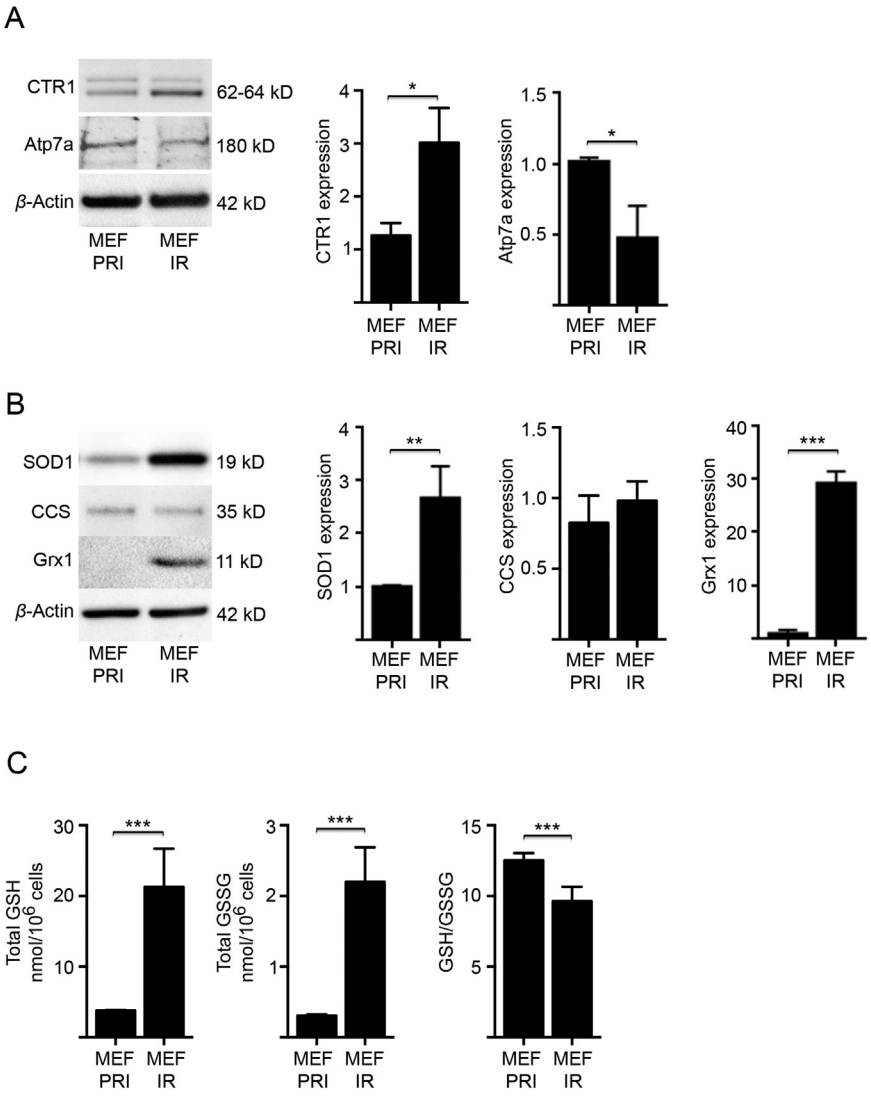

Fig. 2. Senescent cells have altered copper homeostasis and enhanced antioxidant defence mechanisms. **(A)** Expression of key copper homeostasis proteins was analysed in senescent MEFs (MEF IR) at 21 days post-irradiation (IR, 10 Gy) by western blot analyses and densitometry. Expression levels of Ctr1 (major copper import protein) and Atp7a (main copper export protein) were measured in comparison to primary (PRI) MEFs. β-actin was detected as a loading control. **(B)** Expression of key copper dependent proteins was analysed in senescent MEFs (MEF IR) at 21 days post-irradiation (IR, 10 Gy) by western blot analyses and densitometry. Expression levels of superoxide dismutase 1 (SOD1) (antioxidant cuproenzyme), CCS (copper chaperone for superoxide dismutase) and glutaredoxin 1 (Grx1) and were measured in comparison to primary (PRI) MEFs. β-actin was detected as a loading control. **(C)** Senescent MEFs (MEF IR) have elevated intracellular glutathione. Reduced (GSH) and oxidized (GSSG) glutathione were measured in primary (MEF PRI) and senescent MEFs (MEF IR) at 21 days post-irradiation (10 Gy) by HPLC. The GSH:GSSG ratio is also compared. Statistical analysis was performed by student-*t*-test: significant ($*p < 0.05$, $**p < 0.01$, $***p < 0.001$). Data represented as mean ± SD ($n = 3$).

(A)] MEFs were cultured for an additional 11 days to allow for a net change in intracellular copper to occur (Fig. 3**D(ii)**). As expected, non-irradiated primary *Mo*^{br} MEFs (MEF-Mo^{br} PRI) containing the wt*Atp7a* mutation had markedly elevated levels of intracellular copper as a baseline (Fig. 3**D(ii)**). When made senescent, these *Mo*^{br} MEFs (MEF-Mo^{br} IR) further accumulated intracellular copper (~ 2-fold) (Fig. 3**D (ii)**), surpassing levels previously observed in all other senescent cell lines (Fig. 1).

Serially passaged primary *Mo*^{br} MEFs displayed a remarkably similar senescence induction profile to wild-type MEFs (agouti or C57BL/6) (Fig. 3**E(i)**). Additionally, copper accumulation in replicative senescent *Mo*^{br} MEFs (observed at passage 7) was comparable to that observed in irradiated senescent *Mo*^{br} MEFs (Fig. 3**D, E(ii)**). Therefore, it is unlikely that elevated intracellular copper elicits more rapid induction or transition to cellular senescence. Previously, several groups demonstrated premature senescence in human fibroblasts induced through treatment with high copper concentrations (250 and 500 μM $CuSO_4$) [8,47,48]. Copper-induced cellular senescence was likely driven through ROS generation [8], but did not occur in primary *Mo*^{br} MEFs (passage 4) despite these cells containing at least six-fold more intracellular copper (Fig. 3**D**). This may be due to adaptation of the *Mo*^{br} MEFs to manage the gradual build-up of copper in these cells, in contrast to the acute stress imposed by treatment with high levels of copper [8]. Taken together, these results suggest that enhanced copper levels do not necessarily drive senescence.

3.4. Senescence-associated copper accumulation is linked to impaired autophagic-lysosomal function

We previously demonstrated that autophagic-lysosomal degradation is impaired in senescent cells, contributing to iron dyshomeostasis (impaired ferritinophagy) [44]. We therefore explored whether the preservation of autophagic-lysosomal degradation in senescent cells was sufficient to prevent copper accumulation. Rapamycin, an mTOR inhibitor [35], activates autophagy and preserves lysosomal function in senescent cells [68]. We treated primary MEFs with rapamycin (100 nM) while they were irradiated (10 Gy) to undergo senescence and sustained this treatment for 10 days. Cell culture medium was changed twice over this time period and rapamycin treatment was maintained with each medium change. Note that 10 days of culturing post-irradiation (10 Gy) is sufficient to achieve > 80% senescence in MEF cultures (Fig. 1**A**). The LC3 protein in its lipidated form (LC3-II) normally builds up in autophagosomes of cells and is degraded by lysosomal proteases following autophagosome-lysosome fusion [51,70]. Thus, the persistent accumulation of LC3-II in senescent cells indicates impairment in lysosomal degradation and the resultant accumulation of autophagosomes [44,70]. We therefore assessed LC3-II levels in rapamycin treated irradiated MEFs 10 days post-irradiation and found that levels of LC3-II were decreased, indicating that autophagic-lysosomal degradation in rapamycin treated cells was preserved post-irradiation (Fig. 4**A**). In addition to decreased LC3-II, the phosphorylated form of

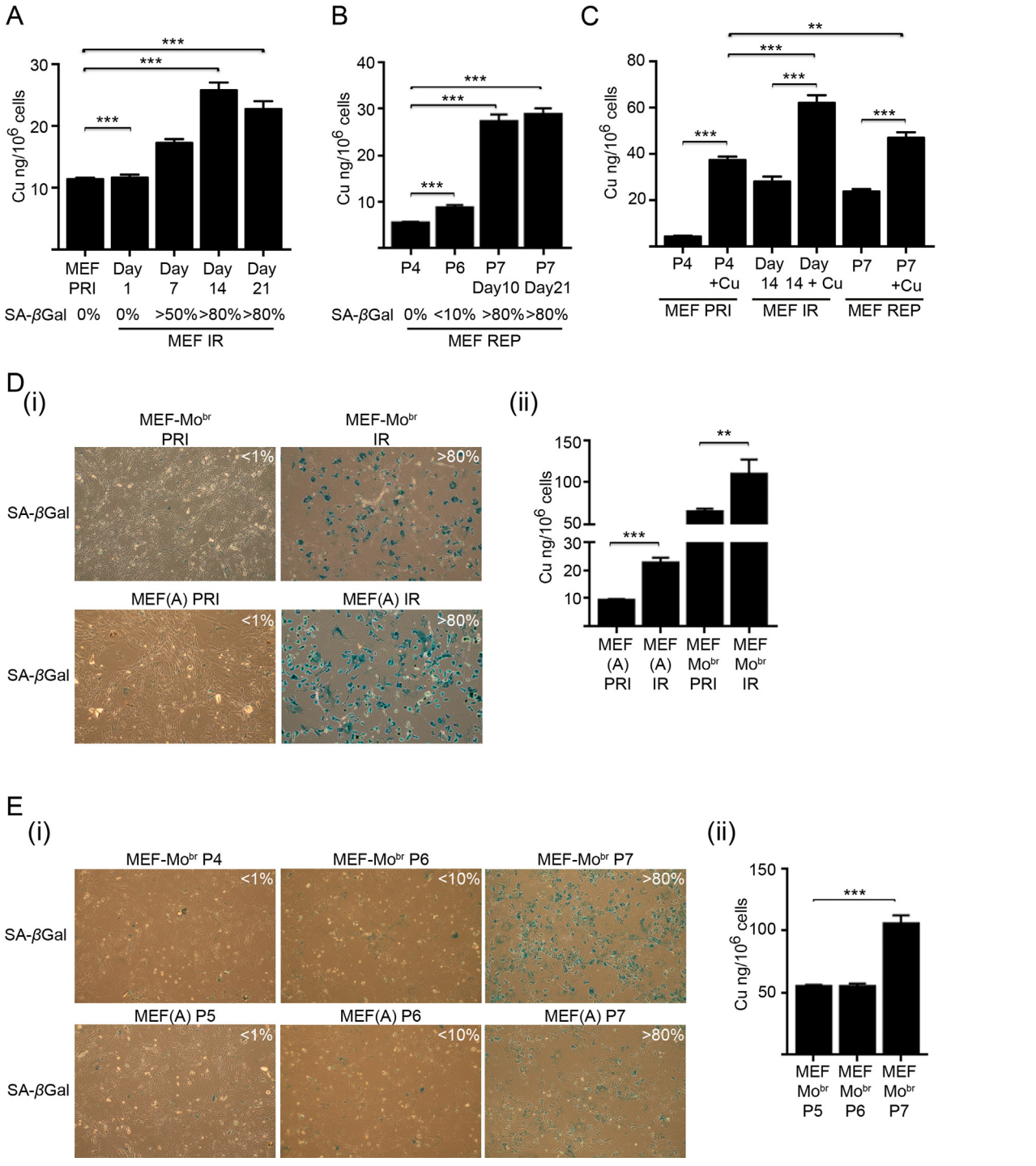

(caption on next page)

ribosomal protein S6 (pS6), a well-established marker of mTOR activation, also was diminished in rapamycin treated irradiated MEFs (Fig. 4**A**). This observation was consistent with potentially enhanced autophagy through the inhibition of mTOR [7]. These results suggest that rapamycin treatment preserved the autophagic-lysosomal degradation pathway in irradiated MEFs. Next, we assessed intracellular copper levels in rapamycin treated irradiated MEFs and found a significant reduction in copper levels compared to untreated (basal) irradiated MEFs (Fig. 4**B**). In addition, once senescence was fully established (10 days post-irradiation), subsequent rapamycin treatment (100 nM for 4 days) mitigated intracellular copper accumulation (Fig. 4**C**). However, when we assessed Atp7a levels in rapamycin treated irradiated MEFs 10 days post-irradiation, we found that the level of Atp7a was further diminished, possibly as a result of activated autophagic-lysosomal degradation **(**Fig. 4**D)**. Atp7a, analogous to the related Atp7b, is likely to be degraded via the lysosomal and proteasomal pathways [45]**;** however, senescent cells lack efficient lysosomal function [68]. Taken together these data suggest that copper accumulation in senescent MEFs was linked to an impaired autophagic-lysosomal function and not a consequence of reduced Atp7a levels. One possible mechanism to explain the copper accumulation is that copper builds up in endocytic structures such as autophagosomes, multivesicular bodies (MVB), or amphisomes. Autophagosomes can fuse with MVBs and endosomes to generate amphisomes prior to fusion with

Fig. 3. Copper accumulation in senescent cells is saturable and limited by Atp7a. **(A)** Copper accumulation in irradiated (10 Gy) senescent MEFs (MEF IR) over prolonged culturing. ICP-MS analyses demonstrated cumulative intracellular copper accumulation in irradiated (10 Gy) senescent MEFs (MEF IR) over the culturing time points indicated (day 1, 7, 14 and 21). Note that copper accumulation plateaued after day 14. Baseline intracellular copper levels in primary MEFs (MEF PRI) are also shown. Percentage of senescent MEFs (MEF IR) over the culturing time points indicated as SA-βgal positive activity. **(B)** Copper accumulation in MEFs undergoing replicative senescence (MEF REP). ICP-MS analyses demonstrated that copper accumulated when replicative senescence commenced ($<$ 10%) at passage 6 and was augmented with senescence enrichment ($>$ 80%) at passage 7. Note copper accumulation plateaued after culturing passage 7 senescent MEFs for 10 days ($\sim$ 5-fold) following which no further increase in copper was reported at day 21. Percentage of senescent MEFs in continually passaged cultures (passages 4, 6 and 7) is indicated as percentage of cells with SA-βgal activity. **(C)** Capacity of senescent MEFs to accumulate copper is dependent on extracellular copper concentration. Irradiated senescent MEFs (MEF IR, 14 days post irradiation) and replicative senescent MEFs (MEF REP P7, day 10), were cultured for 24 h in basal medium, or media supplemented with 20 μM copper (as $CuCl_2$). ICP-MS analyses revealed a greater increase in accumulated copper in IR senescent MEFs compared to replicative senescent MEFs following copper treatment. The baseline and copper supplemented intracellular Cu level in primary (PRI) MEFs (P4) is also shown. **(D)** Senescent irradiated Mottled Brindled (*Mo^{br}*) MEFs accumulate substantial copper compared to senescent agouti MEFs. **(i)** Sub-lethal gamma irradiation (10 Gy) caused the majority ($>$ 80%) of *Mo^{br}* (MEF Mo^{br} IR) and agouti MEFs[MEF (A) IR] to display positive SA-βgal activity 10 days post-irradiation. Images were taken at 100X magnification. **(ii)** ICP-MS analyses demonstrated that senescent *Mo^{br}* MEFs (MEF Mo^{br} IR) accumulated intracellular copper ($\sim$ 2-fold) at 21 days post-irradiation compared to primary *Mo^{br}* MEFs (MEF Mo^{br} PRI). Intracellular copper levels of primary and irradiated senescent agouti MEFs are shown for comparison. Note that intracellular copper in non-irradiated primary *Mo^{br}* MEFs (MEF Mo^{br} PRI) was highly elevated compared to wild type MEFs of C57BL/6 or agouti background. **(E)** Replicatively senescent Mottled Brindled (*Mo^{br}*) MEFs accumulate substantial copper post senescence induction. **(i)** Primary (non-immortalized) *Mo^{br}* and agouti MEFs were induced to senescence by replicative exhaustion. Senescent cell population in culture was determined through staining for senescence-associated beta-galactosidase (SA-βgal) activity (blue staining). Note that primary *Mo^{br}* and agouti MEFs underwent replicative exhaustion at passage 7 under our culturing conditions. More than 80% of cells stained positive for SA-βgal activity when cultured for a minimum of 10 days following senescence induction. Images were taken at 100 × magnification. **(ii)** ICP-MS analyses demonstrated that replicatively senescent *Mo^{br}* MEFs (MEF Mo^{br} P7) accumulated intracellular copper ($\sim$ 2-fold) at 21 days post senescence induction compared to primary Mo^{br} MEFs (MEF Mo^{br} PRI). Statistical analysis was performed by student-*t*-test: significant ($^{*}p < 0.05$, $^{**}p < 0.01$, $^{***}p < 0.001$). Data represented as mean ± SD ($n = 3$).

lysosomes [26]. Autophagosomes, MVBs, or amphisomes may thus serve as temporary sinks for elevated copper in non-senescent cells. Subsequent export of copper then may occur through fusion of amphisomes/autophagosomes with the lysosome, followed by exocytic fusion of the resultant auto-lysosome with the plasma membrane to release the copper [14]. However, in senescent cells, due to lack of lysosomal turnover of these structures, these accumulating autophagosomes/ MVBs/amphisomes may continue to sequester copper, functioning as a reservoir of copper. In support of this hypothesis, intracellular multivesicular compartments have been observed to accumulate in ATP7B-expressing CHO-K1 cells under conditions of elevated copper [38]. ATP7B, a P_{1B}-type transmembrane ATPase similar to Atp7a but expressed highly in hepatocytes, is involved in copper export and is localized to these compartments, suggesting that it may traffic copper to these MVBs [57]. As we did not detect any expression of *Atp7b* transcript in primary or senescent MEFs (not shown) it is possible that Atp7a follows a similar pathway in these cells. The further copper accumulation seen in Atp7a deficient *Mo^{br}* MEFs combined with that observed in autophagy-impaired senescent cells, suggests that efficient copper export requires both functional Atp7a and autophagic-lysosomal function. This is supported by the cumulative effect on copper levels observed in senescent *Mo^{br}* MEFs (Fig. 3**D (ii)**).

To test this hypothesis we treated primary MEFs with the lysosome inhibitor bafilomycin A1 (Baf) with the aim of phenocopying, to a limited extent, the effects of perturbed autophagic-lysosomal degradation observed in senescent MEFs. Treating primary MEFs with Baf led to a concomitant build-up of LC3-II levels (Fig. 4**E**), similar to our observations of lysosomal impairment in senescent MEFs (Fig. 4**A**). Interestingly, impairment of the autophagic-lysosomal degradation pathway in primary MEFs treated for 16 h with 20 μM $CuCl_2$ and Baf, led to a significant accumulation of copper, indicating the important role of lysosomes in the export of copper from MEFs (Fig. 4**F**). Note that Baf was previously shown to induce endosomal accumulation of Atp7a as a consequence of perturbed endosomal recycling, which may also contribute to the increased copper levels observed in primary cells treated with Baf [56]. Thus, preservation and possible restoration of autophagic-lysosomal function was sufficient to prevent (Fig. 4**B**) and reverse (Fig. 4**C**), respectively, the copper accumulation phenotype in senescent cells.

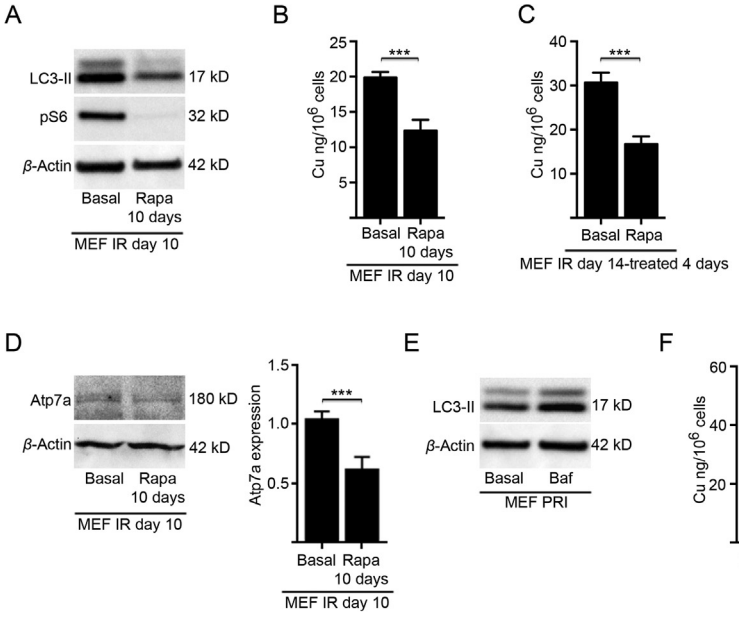

Fig. 4. Rapamycin treatment attenuates senescence-associated copper accumulation. **(A)** Sustained rapamycin treatment preserves autophagic-lysosomal function in irradiated MEFs. Western blot analyses demonstrated that levels of LC3-II and phosphorylated ribosomal protein S6 (pS6) were significantly reduced by sustained treatment of irradiated MEFs for 10 days post-irradiation (10 Gy) with rapamycin (100 nM). β-actin was detected as a loading control. **(B)** Sustained rapamycin treatment limited intracellular copper accumulation in irradiated MEFs. ICP-MS analyses demonstrated that irradiated MEFs subjected to sustained treatment with rapamycin (100 nM) showed markedly reduced copper accumulation at 10 days post-irradiation (10 Gy). **(C)** Rapamycin treatment after senescence establishment reversed intracellular copper accumulation in irradiated MEFs. ICP-MS analyses demonstrated that senescent irradiated MEFs treated with rapamycin (100 nM) for 4 days after senescence establishment (10 days post-irradiation) reversed copper accumulation. Statistical analysis was performed by student-*t*-test: significant ($^{*}p < 0.05$, $^{**}p < 0.01$, $^{***}p < 0.001$). Data represented as mean ± SD ($n = 3$). **(D)** Sustained rapamycin treatment did not enhance Atp7a levels. Western blot analyses and densitometry demonstrated that levels of Atp7a did not increase by sustained treatment of irradiated MEFs for 10 days post-irradiation (10 Gy) with rapamycin (100 nM). β-actin was detected as a loading control. **(E)** Bafilomycin A1 (Baf) treatment attenuates autophagic-lysosomal function in primary MEFs. Western blot analyses demonstrated that the level of LC3-II was significantly elevated by treatment of primary MEFs with Baf (100 nM) for 16 h. β-actin was detected as a loading control. **(F)** Inhibition of autophagic-lysosomal function enhanced intracellular copper accumulation in primary MEFs. Primary MEFs were cultured for 16 h in basal medium, or medium supplemented with 20 μM copper (as $CuCl_2$), with or without Baf A1 (100 nM). ICP-MS analyses revealed a greater increase in accumulated copper in primary MEFs treated with Baf A1 compared to primary MEFs without Baf A1 treatment following 16 h of Cu treatment. The baseline intracellular copper level in primary (PRI) MEFs (P4) is also shown.

4. Conclusion

Our results demonstrate altered copper homeostasis is linked to impaired autophagy in senescent cells. Significantly, this study for the first time establishes a possible connection between Atp7a and the autophagic-lysosomal pathway, indicating a requirement for both for efficient copper export. Our finding that the preservation and re-activation of autophagic-lysosomal function by rapamycin in irradiated MEFs resulted in a concomitant reduction in copper levels suggests a possible and yet undefined association between cellular autophagy, Atp7a and copper export. A model to account for the observations in this study is that lysosomal dysfunction in senescent cells leads to increased Ctr1 and copper sequestration within accumulating autophagosomes/MVBs/amphisomes via a functional Atp7a. This is in contrast to *Mo*^{br} MEFs, where autophagic-lysosomal function is intact but absence of a functional Atp7a leads to an accumulation of intracellular copper (possibly non-compartmentalized). When both autophagic-lysosomal function is impaired and Atp7a is absent in senescent *Mo*^{br} MEFs, copper accumulates even further. Hence, Atp7a likely functions within the autophagic-lysosomal pathway and both are needed for efficient copper export. Notably, in support of our model, Atp7a is known to facilitate copper import in lysosome-related organelles such as melanosomes [64] and phagosomes [75]. Further, the C-terminus of Atp7a harbours a DKHSLL signature that conforms to the dileucine-based motifs, DXXLL or [DE]XXXL[LI], that serve as lysosomal targeting signals [10,58]. While this suggests a specific and direct mode of transport of Atp7a to the lysosomal membrane, the mode of delivery of copper to the lysosome and the role of Atp7a still remains poorly defined. The observation that senescence induction leads to impaired autophagy accompanied by altered copper homeostasis, suggests an important interplay between lysosomal function and copper metabolism. We envisage that understanding this aspect of copper biology will have far reaching consequences in the identification of new molecular targets and development of therapies to combat disorders linked to aberrations in copper metabolism.

Acknowledgments

The authors would like to thank Ms Irene Volitakis (University of Melbourne, Australia) for ICP-MS analyses and Luke Amor from the Deakin University Animal Facility for technical support. The Florey Institute of Neuroscience and Mental Health acknowledges support from the Victorian Government. This study was funded by the National Health and Medical Research Council of Australia (NHMRC) (1027125) (M.A. Cater) and by Deakin University (M.A. Cater, S. La Fontaine).

Author contributions

Masaldan S designed and conducted most of the experiments. Clatworthy SAS and Meggyesy PM helped with data collection. Denoyer D helped prepare and genotyped MEFs from agouti, mottled brindle (*Mo*^{br}) mice. Gamell C helped conduct IR experiments. Smith ZM and Francis PS quantified GSH and GSSG. Cater MA designed, funded and supervised the project. Masaldan S, La Fontaine S, and Cater MA wrote the manuscript.

Appendix A. Supporting information

Supplementary data associated with this article can be found in the online version at http://dx.doi.org/10.1016/j.redox.2018.03.007.

References

[1] A. Andersson-Sjoland, J.C. Karlsson, K. Rydell-Tormanen, ROS-induced endothelial stress contributes to pulmonary fibrosis through pericytes and Wnt signaling, Lab. Investig. 96 (2016) 206–217.

[2] M.P. Baar, R.M. Brandt, D.A. Putavet, J.D. Klein, K.W. Derks, B.R. Bourgeois, S. Stryeck, Y. Rijksen, H. Van Willigenburg, D.A. Feijtel, I. Van Der Pluijm, J. Essers, W.A. Van Cappellen, I.W.F. Van, A.B. Houtsmuller, J. Pothof, R.W. De Bruin, T. Madl, J.H. Hoeijmakers, J. Campisi, P.L. De Keizer, Targeted apoptosis of senescent cells restores tissue homeostasis in response to chemotoxicity and aging, Cell 169 (2017) 132–147 (e16).

[3] D.J. Baker, B.G. Childs, M. Durik, M.E. Wijers, C.J. Sieben, J. Zhong, R.A. Saltness, K.B. Jeganathan, G.C. Verzosa, A. Pezeshki, K. Khazaie, J.D. Miller, J.M. van Deursen, Naturally occurring p16(Ink4a)-positive cells shorten healthy lifespan, Nature 530 (2016) 184–189.

[4] D.J. Baker, T. Wijshake, T. Tchkonia, N.K. Lebrasseur, B.G. Childs, B. Van De Sluis, J.L. Kirkland, J.M. van Deursen, Clearance of p16Ink4a-positive senescent cells delays ageing-associated disorders, Nature 479 (2011) 232–236.

[5] L. Banci, I. Bertini, S. Ciofi-Baffoni, T. Kozyreva, K. Zovo, P. Palumaa, Affinity gradients drive copper to cellular destinations, Nature 465 (2010) 645–648.

[6] L. Belguendouz, L. Fremont, A. Linard, Resveratrol inhibits metal ion-dependent and independent peroxidation of porcine low-density lipoproteins, Biochem Pharmacol. 53 (1997) 1347–1355.

[7] E.F. Blommaart, J.J. Luiken, P.J. Blommaart, G.M. Van Woerkom, A.J. Meijer, Phosphorylation of ribosomal protein S6 is inhibitory for autophagy in isolated rat hepatocytes, J. Biol. Chem. 270 (1995) 2320–2326.

[8] E. Boilan, V. Winant, E. Dumortier, J.P. Piret, F. Bonfitto, H.D. Osiewacz, F. Debacq-Chainiaux, O. Toussaint, Role of p38MAPK and oxidative stress in copper-induced senescence, Age (Dordr) 35 (2013) 2255–2271.

[9] S.D. Bouldin, M.A. Darch, P.J. Hart, C.E. Outten, Redox properties of the disulfide bond of human Cu,Zn superoxide dismutase and the effects of human glutaredoxin 1, Biochem. J. 446 (2012) 59–67.

[10] T. Braulke, J.S. Bonifacino, Sorting of lysosomal proteins, Biochim. Et. Biophys. Acta (BBA)-Mol. Cell Res. 1793 (2009) 605–614.

[11] J. Brose, S. La Fontaine, A.G. Wedd, Z. Xiao, Redox sulfur chemistry of the copper chaperone Atox1 is regulated by the enzyme glutaredoxin 1, the reduction potential of the glutathione couple GSSG/2GSH and the availability of Cu(I), Metallomics 6 (2014) 793–808.

[12] J. Camakaris, D.M. Danks, L. Ackland, E. Cartwright, P. Borger, R.G. Cotton, Altered copper metabolism in cultured cells from human Menkes' syndrome and mottled mouse mutants, Biochem. Genet. 18 (1980) 117–131.

[13] J. Campisi, L. Robert, Cell senescence: role in aging and age-related diseases, Interdiscip. Top. Gerontol. 39 (2014) 45–61.

[14] M.A. Cater, S. La Fontaine, K. Shield, Y. Deal, J.F. Mercer, ATP7B mediates vesicular sequestration of copper: insight into biliary copper excretion, Gastroenterology 130 (2006) 493–506.

[15] M.A. Cater, S. Materia, Z. Xiao, K. Wolyniec, S.M. Ackland, Y.W. Yap, N.S. Cheung, S. La Fontaine, Glutaredoxin1 protects neuronal cells from copper-induced toxicity, Biometals 27 (2014) 661–672.

[16] J. Chang, Y. Wang, L. Shao, R.M. Laberge, M. Demaria, J. Campisi, K. Janakiraman, N.E. Sharpless, S. Ding, W. Feng, Y. Luo, X. Wang, N. Aykin-Burns, K. Krager, U. Ponnappan, M. Hauer-Jensen, A. Meng, D. Zhou, Clearance of senescent cells by ABT263 rejuvenates aged hematopoietic stem cells in mice, Nat. Med. 22 (2016) 78–83.

[17] B.G. Childs, M. Durik, D.J. Baker, J.M. van Deursen, Cellular senescence in aging and age-related disease: from mechanisms to therapy, Nat. Med. 21 (2015) 1424–1435.

[18] S. Courtois-Cox, S.L. Jones, K. Cichowski, Many roads lead to oncogene-induced senescence, Oncogene 27 (2008) 2801–2809.

[19] D. Denoyer, S. Masaldan, S. La Fontaine, M.A. Cater, Targeting copper in cancer therapy: 'Copper That Cancer', Metallomics 7 (2015) 1459–1476.

[20] D. Denoyer, H.B. Pearson, S.A. Clatworthy, Z.M. Smith, P.S. Francis, R.M. Llanos, I. Volitakis, W.A. Phillips, P.M. Meggyesy, S. Masaldan, M.A. Cater, Copper as a target for prostate cancer therapeutics: copper-ionophore pharmacology and altering systemic copper distribution, Oncotarget (2016).

[21] X. Deschenes-Simard, M.F. Gaumont-Leclerc, V. Bourdeau, F. Lessard, O. Moiseeva, V. Forest, S. Igelmann, F.A. Mallette, M.K. Saba-El-Leil, S. Meloche, F. Saad, A.M. Mes-Masson, G. Ferbeyre, Tumor suppressor activity of the ERK/MAPK pathway by promoting selective protein degradation, Genes Dev. 27 (2013) 900–915.

[22] X. Deschenes-Simard, F. Lessard, M.F. Gaumont-Leclerc, N. Bardeesy, G. Ferbeyre, Cellular senescence and protein degradation: breaking down cancer, Cell Cycle 13 (2014) 1840–1858.

[23] R. Di Micco, A. Cicalese, M. Fumagalli, M. Dobreva, A. Verrecchia, P.G. Pelicci, F. Di Fagagna, DNA damage response activation in mouse embryonic fibroblasts undergoing replicative senescence and following spontaneous immortalization, Cell Cycle 7 (2008) 3601–3606.

[24] A.M. Dirac, R. Bernards, Reversal of senescence in mouse fibroblasts through lentiviral suppression of p53, J. Biol. Chem. 278 (2003) 11731–11734.

[25] R. Dringen, Metabolism and functions of glutathione in brain, Prog. Neurobiol. 62 (2000) 649–671.

[26] C.M. Fader, M.I. Colombo, Autophagy and multivesicular bodies: two closely related partners, Cell Death Differ. 16 (2009) 70–78.

[27] J.H. Freedman, M.R. Ciriolo, J. Peisach, The role of glutathione in copper metabolism and toxicity, J. Biol. Chem. 264 (1989) 5598–5605.

[28] A. Freund, R.M. Laberge, M. Demaria, J. Campisi, Lamin B1 loss is a senescence-associated biomarker, Mol. Biol. Cell 23 (2012) 2066–2075.

[29] A. Grimes, C.J. Hearn, P. Lockhart, D.F. Newgreen, J.F. Mercer, Molecular basis of the brindled mouse mutant (Mo(br)): a murine model of Menkes disease, Hum. Mol. Genet. 6 (1997) 1037–1042.

[30] D.M. Harvey, A.J. Levine, P53 alteration is a common event in the spontaneous

immortalization of primary BALB/c murine embryo fibroblasts, Genes Dev. 5 (1991) 2375–2385.
[31] M. Harvey, A.T. Sands, R.S. Weiss, M.E. Hegi, R.W. Wiseman, P. Pantazis, B.C. Giovanella, M.A. Tainsky, A. Bradley, L.A. Donehower, In vitro growth characteristics of embryo fibroblasts isolated from p53-deficient mice, Oncogene 8 (1993) 2457–2467.
[32] Y. Hatori, S. Clasen, N.M. Hasan, A.N. Barry, S. Lutsenko, Functional partnership of the copper export machinery and glutathione balance in human cells, J. Biol. Chem. 287 (2012) 26678–26687.
[33] M.T. Hemann, M. Narita, Oncogenes and senescence: breaking down in the fast lane, Genes Dev. 21 (2007) 1–5.
[34] B.E. Kim, T. Nevitt, D.J. Thiele, Mechanisms for copper acquisition, distribution and regulation, Nat. Chem. Biol. 4 (2008) 176–185.
[35] Y.C. Kim, K.L. Guan, MTOR: a pharmacologic target for autophagy regulation, J. Clin. Investig. 125 (2015) 25–32.
[36] T. Kuilman, C. Michaloglou, W.J. Mooi, D.S. Peeper, The essence of senescence, Genes Dev. 24 (2010) 2463–2479.
[37] S. La Fontaine, S.D. Firth, P.J. Lockhart, H. Brooks, J. Camakaris, J.F. Mercer, Intracellular localization and loss of copper responsiveness of Mnk, the murine homologue of the Menkes protein, in cells from blotchy (Mo blo) and brindled (Mo br) mouse mutants, Hum. Mol. Genet. 8 (1999) 1069–1075.
[38] S. La Fontaine, M.B. Theophilos, S.D. Firth, R. Gould, R.G. Parton, J.F. Mercer, Effect of the toxic milk mutation (tx) on the function and intracellular localization of Wnd, the murine homologue of the Wilson copper ATPase, Hum. Mol. Genet. 10 (2001) 361–370.
[39] G.A. Lang, T. Iwakuma, Y.A. Suh, G. Liu, V.A. Rao, J.M. Parant, Y.A. Valentin-Vega, T. Terzian, L.C. Caldwell, L.C. Strong, A.K. El-Naggar, G. Lozano, Gain of function of a p53 hot spot mutation in a mouse model of Li-Fraumeni syndrome, Cell 119 (2004) 861–872.
[40] J. Lee, J.R. Prohaska, D.J. Thiele, Essential role for mammalian copper transporter Ctr1 in copper homeostasis and embryonic development, Proc Natl. Acad. Sci. USA 98 (2001) 6842–6847.
[41] Y. Li, J. Hu, F. Guan, L. Song, R. Fan, H. Zhu, X. Hu, E. Shen, B. Yang, Copper induces cellular senescence in human glioblastoma multiforme cells through downregulation of Bmi-1, Oncol. Rep. 29 (2013) 1805–1810.
[42] R.M. Llanos, B.X. Ke, M. Wright, Y. Deal, F. Monty, D.R. Kramer, J.F. Mercer, Correction of a mouse model of Menkes disease by the human Menkes gene, Biochim. Biophys. Acta 1762 (2006) 485–493.
[43] E.B. Maryon, S.A. Molloy, J.H. Kaplan, Cellular glutathione plays a key role in copper uptake mediated by human copper transporter 1, Am. J. Physiol. Cell Physiol. 304 (2013) C768–C779.
[44] S. Masaldan, S.A.S. Clatworthy, C. Gamell, P. Meggyesy, A.-T. Rigopoulos, S. Haupt, Y. Haupt, D. Denoyer, P. Adlard, A.I. Bush, M.A. Cater, Iron accumulation in senescent cells is coupled with impaired ferritinophagy and inhibition of ferroptosis, Redox Biol. (2017).
[45] S. Materia, M.A. Cater, L.W. Klomp, J.F. Mercer, S. La Fontaine, Clusterin (apolipoprotein J), a molecular chaperone that facilitates degradation of the copper-ATPases ATP7A and ATP7B, J. Biol. Chem. 286 (2011) 10073–10083.
[46] S. Materia, M.A. Cater, L.W. Klomp, J.F. Mercer, S. La Fontaine, Clusterin and COMMD1 independently regulate degradation of the mammalian copper ATPases ATP7A and ATP7B, J. Biol. Chem. 287 (2012) 2485–2499.
[47] L. Matos, A. Gouveia, H. Almeida, Copper ability to induce premature senescence in human fibroblasts, Age (Dordr) 34 (2012) 783–794.
[48] L. Matos, A.M. Gouveia, H. Almeida, Resveratrol attenuates copper-induced senescence by improving cellular proteostasis, Oxid. Med. Cell. Longev. 2017 (2017) 3793817.
[49] G.P. McDermott, P.S. Francis, K.J. Holt, K.L. Scott, S.D. Martin, N. Stupka, N.W. Barnett, X.A. Conlan, Determination of intracellular glutathione and glutathione disulfide using high performance liquid chromatography with acidic potassium permanganate chemiluminescence detection, Analyst 136 (2011) 2578–2585.
[50] J. Mikula-Pietrasik, P. Sosinska, J. Janus, B. Rubis, M. Brewinska-Olchowik, K. Piwocka, K. Ksiazek, Bystander senescence in human peritoneal mesothelium and fibroblasts is related to thrombospondin-1-dependent activation of transforming growth factor-beta1, Int. J. Biochem. Cell Biol. 45 (2013) 2087–2096.
[51] N. Mizushima, T. Yoshimori, How to interpret LC3 immunoblotting, Autophagy 3 (2007) 542–545.
[52] J.F. Monty, R.M. Llanos, J.F. Mercer, D.R. Kramer, Copper exposure induces trafficking of the menkes protein in intestinal epithelium of ATP7A transgenic mice, J. Nutr. 135 (2005) 2762–2766.
[53] G. Nelson, J. Wordsworth, C. Wang, D. Jurk, C. Lawless, C. Martin-Ruiz, T. Von Zglinicki, A senescent cell bystander effect: senescence-induced senescence, Aging Cell 11 (2012) 345–349.
[54] J. Nikolich-Zugich, Ageing and life-long maintenance of T-cell subsets in the face of latent persistent infections, Nat. Rev. Immunol. 8 (2008) 512–522.
[55] L. Nyasae, R. Bustos, L. Braiterman, B. Eipper, A. Hubbard, Dynamics of endogenous ATP7A (Menkes protein) in intestinal epithelial cells: copper-dependent redistribution between two intracellular sites, Am. J. Physiol. Gastrointest. Liver Physiol. 292 (2007) G1181–G1194.
[56] M.J. Petris, J.F. Mercer, J.G. Culvenor, P. Lockhart, P.A. Gleeson, J. Camakaris, Ligand-regulated transport of the Menkes copper P-type ATPase efflux pump from the Golgi apparatus to the plasma membrane: a novel mechanism of regulated trafficking, EMBO J. 15 (1996) 6084–6095.
[57] E.V. Polishchuk, M. Concilli, S. Iacobacci, G. Chesi, N. Pastore, P. Piccolo, S. Paladino, D. Baldantoni, I.S.C. Van, J. Chan, C.J. Chang, A. Amoresano, F. Pane, P. Pucci, A. Tarallo, G. Parenti, N. Brunetti-Pierri, C. Settembre, A. Ballabio, R.S. Polishchuk, Wilson disease protein ATP7B utilizes lysosomal exocytosis to maintain copper homeostasis, Dev. Cell 29 (2014) 686–700.
[58] E.V. Polishchuk, R.S. Polishchuk, The emerging role of lysosomes in copper homeostasis, Metallomics 8 (2016) 853–862.
[59] S.R. Rittling, Clonal nature of spontaneously immortalized 3T3 cells, Exp. Cell Res. 229 (1996) 7–13.
[60] C.Q. Scheckhuber, J. Grief, E. Boilan, K. Luce, F. Debacq-Chainiaux, C. Rittmeyer, R. Gredilla, B.O. Kolbesen, O. Toussaint, H.D. Osiewacz, Age-related cellular copper dynamics in the fungal ageing model Podospora anserina and in ageing human fibroblasts, PLoS One 4 (2009) e4919.
[61] M.M. Schmidt, R. Dringen, Glutathione (GSH) synthesis and metabolism. Neural Metabolism In Vivo, Springer, 2012.
[62] P.J. Schmidt, M. Ramos-Gomez, V.C. Culotta, A gain of superoxide dismutase (SOD) activity obtained with CCS, the copper metallochaperone for SOD1, J. Biol. Chem. 274 (1999) 36952–36956.
[63] M. Serrano, A.W. Lin, M.E. Mccurrach, D. Beach, S.W. Lowe, Oncogenic ras provokes premature cell senescence associated with accumulation of p53 and p16INK4a, Cell 88 (1997) 593–602.
[64] S.R.G. Setty, D. Tenza, E.V. Sviderskaya, D.C. Bennett, G. Raposo, M.S. Marks, Cell-specific ATP7A transport sustains copper-dependent tyrosinase activity in melanosomes, Nature 454 (2008) 1142–1146.
[65] W.C. Singleton, K.T. Mcinnes, M.A. Cater, W.R. Winnall, R. Mckirdy, Y. Yu, P.E. Taylor, B.X. Ke, D.R. Richardson, J.F. Mercer, S. La Fontaine, Role of glutaredoxin1 and glutathione in regulating the activity of the copper-transporting P-type ATPases, ATP7A and ATP7B, J. Biol. Chem. 285 (2010) 27111–27121.
[66] Z.M. Smith, J.M. Terry, N.W. Barnett, L.J. Gray, D.J. Wright, P.S. Francis, Enhancing permanganate chemiluminescence detection for the determination of glutathione and glutathione disulfide in biological matrices, Analyst 139 (2014) 2416–2422.
[67] M. Storer, A. Mas, A. Robert-Moreno, M. Pecoraro, M.C. Ortells, V. Di Giacomo, R. Yosef, N. Pilpel, V. Krizhanovsky, J. Sharpe, W.M. Keyes, Senescence is a developmental mechanism that contributes to embryonic growth and patterning, Cell 155 (2013) 1119–1130.
[68] H. Tai, Z. Wang, H. Gong, X. Han, J. Zhou, X. Wang, X. Wei, Y. Ding, N. Huang, J. Qin, J. Zhang, S. Wang, F. Gao, Z.M. Chrzanowska-Lightowlers, R. Xiang, H. Xiao, Autophagy impairment with lysosomal and mitochondrial dysfunction is an important characteristic of oxidative stress-induced senescence, Autophagy 13 (2017) 99–113.
[69] V. Tamboli, A. Defant, I. Mancini, P. Tosi, A study of resveratrol-copper complexes by electrospray ionization mass spectrometry and density functional theory calculations, Rapid Commun. Mass Spectrom. 25 (2011) 526–532.
[70] I. Tanida, N. Minematsu-Ikeguchi, T. Ueno, E. Kominami, Lysosomal turnover, but not a cellular level, of endogenous LC3 is a marker for autophagy, Autophagy 1 (2005) 84–91.
[71] J.M. Terry, J.L. Adcock, D.C. Olson, D.K. Wolcott, C. Schwanger, L.A. Hill, N.W. Barnett, P.S. Francis, Chemiluminescence detector with a serpentine flow cell, Anal. Chem. 80 (2008) 9817–9821.
[72] G.J. Todaro, H. Green, Quantitative studies of the growth of mouse embryo cells in culture and their development into established lines, J. Cell Biol. 17 (1963) 299–313.
[73] J.M. van Deursen, The role of senescent cells in ageing, Nature 509 (2014) 439–446.
[74] J. Wang, H. Geiger, K.L. Rudolph, Immunoaging induced by hematopoietic stem cell aging, Curr. Opin. Immunol. 23 (2011) 532–536.
[75] C. White, J. Lee, T. Kambe, K. Fritsche, M.J. Petris, A role for the ATP7A copper-transporting ATPase in macrophage bactericidal activity, J. Biol. Chem. 284 (2009) 33949–33956.
[76] P.C. Wong, D. Waggoner, J.R. Subramaniam, L. Tessarollo, T.B. Bartnikas, V.C. Culotta, D.L. Price, J. Rothstein, J.D. Gitlin, Copper chaperone for superoxide dismutase is essential to activate mammalian Cu/Zn superoxide dismutase, Proc. Natl. Acad. Sci. USA 97 (2000) 2886–2891.
[77] Y. Zhu, T. Tchkonia, T. Pirtskhalava, A.C. Gower, H. Ding, N. Giorgadze, A.K. Palmer, Y. Ikeno, G.B. Hubbard, M. Lenburg, S.P. O'hara, N.F. Larusso, J.D. Miller, C.M. Roos, G.C. Verzosa, N.K. Lebrasseur, J.D. Wren, J.N. Farr, S. Khosla, M.B. Stout, S.J. Mcgowan, H. Fuhrmann-Stroissnigg, A.U. Gurkar, J. Zhao, D. Colangelo, A. Dorronsoro, Y.Y. Ling, A.S. Barghouthy, D.C. Navarro, T. Sano, P.D. Robbins, L.J. Niedernhofer, J.L. Kirkland, The Achilles' heel of senescent cells: from transcriptome to senolytic drugs, Aging Cell 14 (2015) 644–658.